Economic Analysis of Power Grid Interconnections Among Europe, North-East Asia, and North America With 100% Renewable Energy Generation

Wu, Cong; Zhang, Xiao-ping; Sterling, Michael J. H.

DOI:
10.1109/OAJPE.2021.3085776

Citation for published version (Harvard):
Wu, C, Zhang, X & Sterling, MJH 2021, 'Economic Analysis of Power Grid Interconnections Among Europe, North-East Asia, and North America With 100% Renewable Energy Generation', *IEEE Open Access Journal of Power and Energy*, vol. 8, pp. 268-280. https://doi.org/10.1109/OAJPE.2021.3085776

Received 20 January 2021; revised 30 March 2021; accepted 25 May 2021.
Date of publication 3 June 2021; date of current version 28 June 2021.

Digital Object Identifier 10.1109/OAJPE.2021.3085776

Economic Analysis of Power Grid Interconnections Among Europe, North-East Asia, and North America With 100% Renewable Energy Generation

CONG WU, XIAO-PING ZHANG (Fellow, IEEE), AND MICHAEL J. H. STERLING

Department of Electronic, Electrical and Systems Engineering, School of Engineering, University of Birmingham, Birmingham B15 2TT, U.K.
CORRESPONDING AUTHOR: X.-P. ZHANG (x.p.zhang@bham.ac.uk)

This work was supported in part by the Engineering and Physical Sciences Research Council (EPSRC) under Grant EP/N032888/1 and Grant EP/L017725/1.

ABSTRACT In this paper, we investigate whether the interconnection of power grids with 100% renewable energy generation can bring greater economic benefits now that the technology exists for high power, long distance Ultra High Voltage Direct Current transmission. Based on multi-year historical weather data and demand series, this study compares eight interconnection schemes for three regional grids in Europe, North-East Asia, and North America where there is around 8-hour time difference between any of the two regions. Sensitivity analyses are presented with respect to infrastructure capital cost and different weather year which show that interconnection yields a reduction of approximately 18% in the total annual system cost. The results in this paper also indicate that the regional levelized cost of electricity (LCOE) drops by 31%, 10%, and 10% for Europe, North-East Asia and North America, respectively. It is concluded that there is a strong incentive through both annual cost saving and regional LCOE drop in favour of full long-distance interconnections between the three regions in the context of the international drive towards a net-zero strategy.

INDEX TERMS Transcontinental electricity interconnection, ultra high voltage direct current (UHVDC), renewable energy sources, electricity storage, economic analysis, time difference dependent complementary characteristics, sensitivity analysis.

I. INTRODUCTION

THE current transformation of electrical power grids has been driven by the desire to reduce carbon emissions and has seen a growing proportion of 'renewable', especially wind and solar based [1], [2]. Ever more demanding targets for lower carbon emissions raise the prospect of an electricity sector that could be 100% renewable energy sourced [3], [4] but the recent development of ultra-high voltage (UHV) transmission [5], [6] brings the potential for long distance international interconnection [7], [8].

Many studies examined whether expected demand could be matched by high penetration renewable energy (RE), from national scope [9]–[12] to regional scope [13]–[17], from only power sector [9], [10], [12]–[17] to all energy sectors [3], [4], [18], [19]. The feasibility and viability of such a clean system was discussed comprehensively in [20], [21]. Most studies incorporated the full year hourly dispatch to better accommodate volatile powers from RE sources based on a weather-driven modelling approach. Long-distance transmission raises the possibility of alleviating the fluctuation and intermittency of RE sources by utilizing the smoothing and complementary effects of a large geographical scale.

The concept of grid interconnections was proposed in the early 1980s [22] and there were relevant slow developments [23]–[25] where simplified methodologies were normally employed. In recent years, developments in High Voltage Direct Current (HVDC) power transmissions have given a new impetus to this idea [5], [6], [26]. The interconnector investments for integrating variable RE in Europe at hourly temporal resolution has been estimated [27], [28]. In [29] the challenges and opportunities of exporting renewable generation from Russia to Europe has been examined. Three potential routes for connecting Europe with China and the techno-economic analysis of connecting Europe with North America via a submarine power cable were studied in [30], [31]. The backbone grid scenarios from a global perspective as well as regional schemes were released by GEIDCO [32], e.g., the North America transmission proposal was reported recently [33]. Practical EuroAsia interconnector linking Israel to Europe is under construction [34]. A review on the benefits and challenges of global power grids was provided in [35]. Recently, the feasibility of global electricity network structured in 13 regions was comprehensively studied by CIGRE Working Group C1.35 [36]. Nevertheless, the penetration of RE in electricity systems above is relatively low and it would be a different story for a 100% RE in the future. The 'Desertec' plan for connecting Europe with Mediterranean region was proposed in [13]. Additionally, the feasibility of powering Europe and America with 100% renewable energy has been studied respectively [15], [16]. Both considered the regional grid interconnections and conducted their analysis at high spatial and temporal resolution. So far, however, very few studies explore the economic benefits of multi-continental grid interconnections with 100% RE supply using mass detailed statistics of weather data at high spatial resolution.

Recognising that Europe, North-East Asia (NE_Asia), and North America (N_America) are the three major continental load centers in Europe, Asia and America and the time difference between any two of them is around 8 hours, long distance UHVDC technology now makes the interconnection technically possible. This study aims to investigate whether the interconnection between 100% RE based power grids in Europe, NE_Asia, and N_America can make economic sense (see Table 4 in Appendix for detailed geographical scope). Solar photovoltaics (PV), onshore and offshore wind, and hydro generation along with storage systems are considered to power the three-region system, which are commonly recognized as the most important energy sources by several independent research groups [3], [4], [11], [12], [17]. The major contributions include:

A. GENERATION OF DETAILED RENEWABLE GENERATION SERIES DATA

A number of studies concerning 100% RE used the weather data to generate RE power series (e.g. [9], [10]), however, hardly any of them produce the series based on mass raw data at high temporal and geographical resolution ($0.25° \times 0.25°$) for up to seven years. To obtain the regional profiles of hourly RE generation, we convert 7-year historical weather data within NE_Asia, Europe, and N_America (consisting of nearly 64000 raster cells overall) into solar, onshore and offshore wind power series, respectively. Using two weight-based aggregation formulas and one density-based cluster algorithm, we sort, select and aggregate the power series in raster cells with 50% highest capacity factor into regional series and further select the representative series for each month.

B. GENERATION OF DETAILED DEMAND AND HYDRO SERIES DATA

Hitherto electricity demand series were mainly generated by either scaling historical statistics of a single year (e.g. [15], [17]) or calculating based on synthetic load data (e.g. [14], [16]). In this study, multi-year historical hourly demand series and monthly hydro generation as well as alternatively representative series for long-term planning are retrieved from official websites and used to generate regional representative demand and hydro series.

C. MINIMUM ANNUAL SYSTEM COST OPTIMIZATION MODEL WITH THE DETAILED SERIES DATA

With minimum annual system cost, an optimization model incorporating power dispatch to determine the additional capacities of transmission interconnectors, electricity storage systems, and RE sources is constructed based on the existing installations in 2030 and the expected demands in 2050. Hourly power balance between supply and demand during 12 months (each with four weeks) in the whole system of Europe, NE_Asia, and N_America is selected to represent fully hourly modelling of the entire year.

D. EVALUATION OF INTERCONNECTION SCHEMES BETWEEN THE 3 REGIONS

A few studies looking into transcontinental electricity interconnection have recently appeared [16], [31], however, none of them investigated the different interconnection schemes among three major load centers in the world. Eight schemes are compared from the perspectives of system annual costs and regional levelized cost of electricity in this study.

E. SENSITIVITY ANALYSIS

Sensitivity analysis is conducted from two aspects to investigate the robustness of the results: 1) by varying infrastructure capital cost per unit and 2) by using different individual weather year.

F. ASSESSMENT OF 3-REGION INTERCONNECTION BENEFITS WITH RESPECT TO AROUND 8-HOUR TIME DIFFERENCE

There is around an 8-hour time difference between any two of the 3 regions, and this complementary characteristic is investigated for the first time in this paper.

Section II below shows how the detailed generation and demand time series are generated. Section III shows the minimum annual system cost optimization model incorporating power dispatch to determine the additional capacities of transmission interconnectors, storage systems, and RE sources together with a sensitivity analysis. Section IV presents the results and analysis with our conclusions in Section V. Table 4 $\sim$ 12 and Figure 4 $\sim$ 6 are shown in the Appendix.

II. BASIC DATA

A. HOURLY TIME SERIES OF WIND/SOLAR POWER

Hourly available power of wind/solar powers are converted from historical weather data based on a similar method to that proposed in [37] using 'Atlite' and widely applied in [9], [17], [38], [39]. All the data processing in this section are coded with Python on an IntelCore-i5-8300H/2.3GHz personal laptop with 8G memory.

1) DOWNLOADING WEATHER DATASETS

Seven-year (2011-2017) historical weather data with spatial resolution of 0.25° × 0.25° (approximate 31km × 31km) and temporal resolution of 1 hour is taken from ERA5 datasets, produced by the European Centre for Medium-Range Weather Forecasts (ECMWF)[40]. The water depth of the marine area is obtained from the General Bathymetric Chart of the Oceans (GEBCO) and National Centers for Environmental Information (NCEI) [41]. As a result, there will be a total of 12455 (1566 in marine area) raster cells for Europe, those for NE_Asia and N_America are 24032 (915) and 27246 (1541), respectively.

The mass weather data are downloaded for each sub-area instead of the whole region, i.e. each country in Europe, each province in NE_Asia or each state in N_America, based on the high-resolution geographical shape files of administrative boundaries from the Database of Global Administrative Areas (GADM) [42] and Natural Earth dataset [43]. Downloading seven-year weather data for Europe, NE_Asia and N_America including marine areas takes about 80 h, 125 h, and 144 h respectively through official Climate Data Store Application Program Interface (CDS API), which takes up approximately 393Gb, 450Gb and 422Gb of the storage space.

2) CONVERTING AND AGGREGATING OF DATA

In each sub-area, the seven-year historical weather data is first converted to wind and solar power series in each raster cell. Next, 50% of the raster cells with highest average seven-year capacity factors (CF) are sorted, selected, and aggregated into 5 groups with an interval of 10%. This takes around 10h, 21h, and 20h for Europe, NE_Asia, and N_America, respectively.

The converted power series are then aggregated to sub-area level as (1). It is assumed that 0-10% and 10%-20% of the raster cells with highest average CF are weighted by 0.3, 20%-30% of the cells with highest CF are weighted by 0.2, and last 30%-40% and 40%-50%of the cells are weighted by 0.1 [16].

$$cf^{S}_{r,s,t} = \sum\nolimits_{i=1}^{5} w^{S}_{i}\left(\frac{p_{r,s,i,t}}{c_{r,s,i}}\right)t \in [1, T_{max}] \qquad (1)$$

where $p_{r,s,i,t}$is the aggregated power of group i in sub-area s of region r at hour t for each RE technology and $c_{r,s,i}$is the aggregated capacity. $w^{S}_{i}$and $cf^{S}_{r,s,t}$are the weight and equivalent CF series for sub-area s of region r, respectively. $T_{max} = 61320$ represents the total number of hours for 7 years.

Thereafter, the hourly power series are actually expressed as CF time series.

3) WIND AND SOLAR CONVERTING MODEL

The Enercon E-101 model of wind turbines with rated capacity of 3050 kW and 150 m hub height was used to generate onshore wind power series and the NREL Reference Turbine with 5 MW at 90 m was employed to generate offshore power series, whose power curve is obtained from wind turbine repository from open platform [44]. The original power curve is further improved to account for the smoothing effects of wind speed within each cell by Gaussian kernel [37].

A CdTe-based PV model with fixed tilt angle optimized by the cell's latitude was chosen to generate solar power, which is presented by Huld [45] to estimate the energy yield of PV modules based on irradiance and temperature. See reference [38] for more details about wind and solar converting model.

4) INSTALLING POTENTIAL OF SUB-AREA

In each sub-area, it is assumed that up to 6% of the land area can be covered by PV cells and 10% of the marine area can be covered by offshore wind farms, while only 4% for onshore wind farms due to the societal constraints [4].

The installation density of onshore, offshore wind turbines and PV cells are assumed to be 10 MW/km^2, 10 MW/km^2, and 81.8 MW/km^2, respectively [3], [39]. Additionally, offshore wind turbines are restricted to installation on sites with maximum 50m sea depth [15], [17]. The results are shown in Table 5.

5) REGIONAL POWER SERIES

The equivalent regional power series (Europe, NE_Asia, and N_America) are calculated by the weighted sum of equivalent CF series of sub-areas, taking installing potential as the weight.

$$cf^{R}_{r,t} = \sum\nolimits_{s=1}^{N_r} w^{R}_{r,s} cf^{S}_{r,s,t} t \in [1, T_{max}]\,(2) \qquad (2)$$

where w^{R}_{s}denotes the weight, expressed as the installing potential of sub-area s over the total potential in region r; $cf^{R}_{r,t}$ is the equivalent CF series for region r that consists of N_r sub-areas.T_{max} represents the total number of hours for 7 years.

6) REPRESENTATIVE TIME SERIES OF EACH MONTH

Four-week long hourly power series, starting from Monday, are sampled from the equivalent 7-year power series and then classified for each month. For example, in January of 2011, there is one piece of hourly power series for PV cells and there will be total of 7 series in 7 years for January. Therefore, a total of 12 month sets, each with 7 elements are formed.

A popular density-based clustering method, called DBSCAN [46], is employed to select one representative power series for each month based on the average CF of each series. By this stage, the representative power series of onshore wind, offshore wind, and solar PV in each month for Europe, NE_Asia, and N_America are finally derived.

B. HOURLY TIME SERIES OF HYDRO POWER

As hydro power is less fluctuating and intermittent than solar/wind power and also for the sake of simplicity, we consider hourly hydro power as dispatchable within the available maximum hydro power capacity of a particular month.

We assume that the available maximum hydro power capacity is a constant during each entire month and it varies over the months depending on the seasons and climate conditions.

Ten-year (2010-2019) historical monthly hydro generation for each sub-area in Europe, NE_Asia and N_America are downloaded from official archives (see Table 6). Using the previous cluster algorithm, the representative monthly generation curve (normalized) is obtained for each sub-area. Based on the assumptions that the CFs of hydro generation in 2050 are similar to those in 2017 and the installed capacities are treated as the weight, regional hydro power series are formed.

The monthly and annual capacity factors of the above four technologies in each region are summarized in Table 7.

C. HOURLY TIME SERIES OF DEMAND

Representative one-year demand series for every Europe countries are from Ten-Year Network Development Plan published by ENTSO-E in 2018. Four-year (2016-2019) hourly demand series for states in the United States are from Energy Information Administration, for provinces in Canada are from local Electricity System Operator (ESO) or adjacent ESO.

Due to the paucity of demand data for every province in China, the method proposed by [9] was employed to generate multi-year hourly demand series based on the monthly demand in 2017 and representative one-day demand series at province level, where Gaussian noise and spline interpolation are applied. For Japan, three-year (2017-2019) hourly demand series were gathered from 9 major power companies' websites and then aggregated on a country level. There is no hourly demand series publicly available for South Korea. It is assumed that the pattern of the demand profile is similar to that in Japan as both are advanced industrialised countries and share similar load characteristics; moreover, the South Korea's electricity consumption takes up only 4% of the total energy consumption in NE_Asia [4], thus such assumption would have limited impact. Likewise, the demand series in North Korea, Russia Far East and Mongolia are assumed to be similar to that of their adjacent Jilin, Heilongjiang and Inner Mongolia in China, respectively.

The sources of historical statistics, along with representative demand series serving for long-term planning for Europe and NE_Asia are listed in Table 6.

Based on gathered demand series for the sub-areas and projected electricity consumption in 2050 including transmission & distribution loss [4], the final regional representative demand series are obtained as previously.

D. KEY PARAMETERS AND FINANCIAL ASSUMPTIONS

The expected installed capacities of RE technologies in 2030, the potential installed capacities and the projected annual demands in 2050 are shown in Table 5. Information about the interconnections among three regions, e.g. locations, distances, types, and transmission losses as well as HVDC transmission interconnector costs are summarized in Table 8 and Table 9. The financial assumptions and key parameters of each technology are listed in Table 10. It should be emphasized herein that the relatively lower projected cost data are used for Solar and Energy Storage, compared to [47]–[49] while the cost data used for UHVDC are taken from recent projects and assumed to be unchanged in the future. Such assumptions for cost data would encourage more local installations of solar and energy storage rather than transmission interconnectors, which will lead to conservative results for interconnections, i.e. lower interconnection capacities.

III. MATHEMATICAL MODELS

A. MODELLING OF RE SOURCES, ELECTRICITY STORAGE SYSTEMS, AND TRANSMISSION INTERCONNECTORS

In order to introduce hourly dispatch of the three-region system into planning model, it is essential to model the operations of commissioned technologies to supply power.

For an electricity system with 100% RE supply, dispatching the power from RE sources whose available outputs rely heavily on the availability of natural resources [50], a basic requirement is to satisfy the demand.

$$p^{RE}_{t,i,j,z} \leq P^{avi}_{t,i,j,z} \tag{3}$$

where $p^{RE}_{t,i,j,z}$, $P^{avi}_{t,i,j,z}$ represent the actual (dispatched) and available power at time t from RE type i during the representative week of month j in region z, respectively.

Deployment of an electricity storage system may contribute to accommodating volatile RE generation [51], [52]. The electricity stored in a certain period, associated with those of its adjacent periods, should meet the requirement of state of charge (SoC). Also, the storage system is assumed to recover its initial SoC when a dispatch cycle ends.

$$\begin{cases} E_{t,j,z} = (1-\tau)E_{t-1,j,z} + (p^{ch}_{t,j,z}\eta_{ch} - p^{dis}_{t,j,z}\big/\eta_{dis})\Delta t \\ E_{0,j,z} = E_{T,j,z} \\ \gamma^{min}\psi^{st}_{z} \leq E_{t,j,z} \leq \gamma^{max}\psi^{st}_{z} \end{cases} \tag{4}$$

where $p^{ch}_{t,j,z}$ and $p^{dis}_{t,j,z}$ represent the charging and discharging powers of the storage at time t during month j in region z. η_{ch} and η_{dis} are the charging and discharging efficiency. Δt denotes the time interval. $E_{t,j,z}$, $E_{t-1,j,z}$, $E_{0,j,z}$, and $E_{T,j,z}$ are, respectively, the electricity stored at times t, t-1, 0, and T (the total hours) in region z, and ψ^{st}_{z} is the installed capacity. γ^{min} and γ^{max} are the minimum and maximum SoC.

A complete HVDC interconnector normally consists of a DC transmission line and two converter stations. Taking the power loss along HVDC line and converter stations into account, both the transmission interconnectors are modelled as follows.

$$p^{end}_{t,j,z,n} = p^{start}_{t,j,z,n}[1 - \left(\delta^{li}L_{z,n} + \delta^{te}\right)] \tag{5}$$

where $p^{start}_{t,j,z,n}$ and $p^{end}_{t,j,z,n}$ denote, respectively, the powers at the starting and ending points of the transmission interconnector at time t during month j with the transfer occurring

TABLE 1. Additional annual costs and regional LCOE of eight schemes.

Scheme	Transmission capacity (GW)			Additional annual costs (billion $)				LCOE($/MWh)					
	L1[a]	L2	L3	Total	Line[c]	Storage	d0/%[d]	Europe	d1/%	NE_Asia	d2/%	N_America	d3/%
0	-[b]	-	-	1021	0.0%	42.3%	-	69.5	-	52.9	-	47.2	-
1	213	-	-	921	1.9%	38.3%	9.8%	49.3	29.1%	51.7	2.3%	47.2	0.0%
2	-	113	-	996	3.1%	39.2%	2.5%	61.8	11.1%	52.9	0.0%	48.3	-2.3%
3	-	-	348	933	4.3%	32.2%	8.6%	69.5	0.0%	49.1	7.2%	41.4	12.3%
4	-	193	456	879	11.9%	30.8%	13.9%	58.5	15.9%	48.0	9.3%	42.1	10.8%
5	224	-	539	836	9.6%	30.3%	18.2%	48.2	30.7%	47.5	10.2%	42.3	10.4%
6	356	181	-	882	9.0%	31.7%	13.7%	47.3	32.0%	49.3	6.9%	46.8	0.8%
7	216	8	527	836	9.6%	30.5%	18.1%	48.1	30.9%	47.6	10.0%	42.3	10.4%

[a]L1, L2, and L3 represent the interconnection of Europe-NE_Asia, Europe-N_America, and NE_Asia-N_America, respectively; [b] '-' under 'Transmission capacity' represents there is no interconnection between the two regions; [c] The annual costs of transmission interconnector and storage system are expressed as a ratio of total system annual costs; [d] 'd_0'-'d_3' is the cost decrease w.r.t respective reference scheme 0.

from region z to region n. $L_{z,n}$ and δ^{li} are the length of transmission interconnector between region z and region n, and the transmission loss correspondingly. $\delta^{te}$is the power conversion loss in converter stations.

B. PLANNING MODEL COUPLED WITH DISPATCH

An integrated optimization model to determine the regional additional capacities of RE sources, storage systems and transmission interconnectors among Europe, NE_Asia, and N_America is proposed, which incorporates hourly dispatch of these facility assets in the whole three-region system. The base year and target year are 2030 and 2050, respectively. The total investment in all additional facilities since 2030 is calculated using the demands of 2050 (assuming no existing transmission interconnectors and large-scale storage systems in 2030). The total cost, expressed as annual cost, consists of a) the annualized overnight capital costs, b) fixed operation and maintenance costs and c) variable operation and maintenance (O&M) costs. The objective function is shown in (6). The constraints include installed capacity limits, power balance, and output limits of facilities.

$$min \begin{Bmatrix} [\sum_{i,z}(CRF_i\psi_{i,z}\omega_{i,z} + \emptyset_i^{\text{fix}}\psi_{i,z}\omega_{i,z}) + \sum\limits_{t,i,z}\emptyset_i^{\text{var}}p_{t,i,z}] \\ +[\sum_{I\in\Omega}(CRF_I\psi_I\omega_I + \emptyset_I^{\text{fix}}\psi_I\omega_I)] \end{Bmatrix} \tag{6}$$

where CFR_i is the capital recovery factors of RE technologies, and energy storage systems, calculated as (7). $\psi_{i,z}$and $\omega_{i,z}$ denote the installed capacity and capital cost per unit of technologies in region z. $\emptyset_i^{\text{fix}}$and $\emptyset_i^{\text{var}}$are the fixed and variable operational and maintenance expenditure of technology i. $p_{t,i,z}$is the power output of technology i in region z at time t. $\sum_{I\in\Omega}(CRF_I\psi_I\omega_I + \emptyset_I^{\text{fix}}\psi_I\omega_I)$ are the interconnector related costs where I denotes an interconnector between a certain pair of regions and Ω is a set including all interconnection routes.

$$CRF_i = WACC(1+WACC)^y/[(1+WACC)^y - 1] \tag{7}$$

where a weighted average cost of capital (WACC) of 7% is set to all technologies and y denotes lifetime.

IV. RESULTS AND ANALYSIS

A. COMPARISON OF EIGHT INTERCONNECTION SCHEMES

Eight schemes based on different interconnection scenarios between Europe, NE_ASIA, and N_America, are compared in terms of total annual system cost and regional LCOE in this study. Table 1 summarizes the additional annual costs along with LCOE. The proposed installed capacities and cost breakdowns are summarized in Table 11 and Table 12. Regional LCOE is calculated using (8)-(11).

$$F_z^{RE} = \sum_i(CRF_i\psi_{i,z}\omega_{i,z} + \emptyset_i^{\text{fix}}\psi_{i,z}\omega_{i,z}) + \sum_{t,i}\emptyset_i^{\text{var}}p_{t,i,z} \tag{8}$$

$$F_z^e = \sum\nolimits_i\left(CRF_i\psi_{i,z}^e\omega_{i,z}^e + \emptyset_i^{\text{fix}}\psi_{i,z}^e\omega_{i,z}^e\right) \tag{9}$$

$$F_z^{line} = \sum\nolimits_n 0.5\Psi_{z,n}^{annual} \tag{10}$$

$$LCOE_z = \frac{F_z^{RE} + F_z^{line} + F_z^e}{E_z^{demand} + E_z^{export} - E_z^{import}} \tag{11}$$

where $\psi_{i,z}^e$and $\omega_{i,z}^e$are the existing installed capacity and capital cost per unit of technology i in 2030. $F_z^e$and $F_z^{line}$are the annual costs of existing RE and interconnectors belonging to region z, respectively. It should be clarified that the annual cost of existing RE sources is calculated using the capital cost in 2030. It is assumed that two regions being connected share the investment costs of transmission interconnector evenly, calculated by (9), where $\Psi_{z,n}^{annual}$represents the discounted annual cost of the transmission interconnector connecting region z and region n. E_z^{export} and E_z^{import} are the annul accumulated export and import electricity.

In Table 1, from both the perspectives of the whole system and regional system, the interconnection will yield a reduction for all cost metrics. Specifically, the interconnection will decrease the annual cost of the whole system by up to 18% in scheme 5 and 7, and also decrease the LCOE of Europe, NE_Asia, and N_America by around 31%, 10% and 10%, respectively. The reason why the annual cost decreases is that the interconnection reduces the overall installations of RE sources and storage systems in the grids (Table 12). Besides, the scheme that has lower annual cost does not mean a lower regional LCOE for all the regions because the calculation of

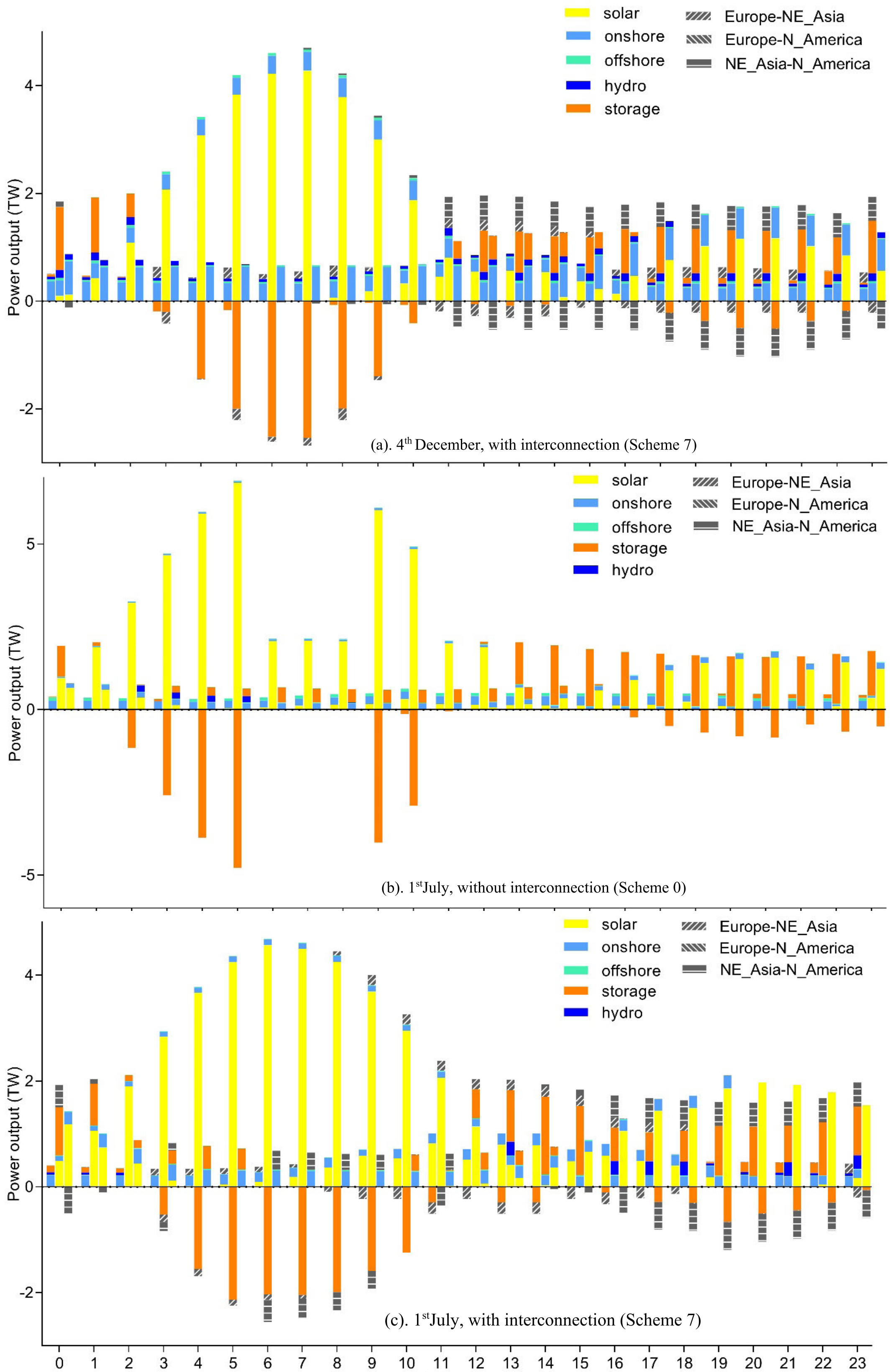

FIGURE 1. **Hourly power in the whole three region system (a segment of 24 hours).**

LCOE further involves regional electricity import and export, as well as existing installations in 2030.

In addition, Scheme 5 and Scheme 7 have similar results in every cost metric, which indicates the interconnection between Europe and N_America plays a less important role in cost reductions. Although the annual cost of Scheme 7 is 0.07% higher than that of Scheme 5, Scheme 7 is selected as the optimal scheme considering its more supply options at minor additional costs. It is observed that N_America has lowest LCOE (47.2 \$/MWh) before interconnection compared to Europe (69.5 \$/MWh) and NE_Asia (52.9 \$/MWh), the value will drop to 42.3 \$/MWh after transmission interconnectors are in place, which shows a win-win situation for all the participants. Additionally, investment in transmission interconnectors takes up only a small share out of the total annual cost, less than 10% in most schemes. Last, schemes with at least two interconnections perform better in terms of the annual cost reductions than those with only a single one.

B. EXCHANGE OF HOURLY POWER AND MONTHLY ELECTRICITY

Hourly power contributions from different technologies under Scheme 7 and Scheme 0 are shown in Fig. 1 where Fig. 1(a), 1(b) and 1(c) are for Scheme 7 on 4th Dec, Scheme 0 on 1st July, Scheme 7 on 1st July, respectively. Three bars in each time interval corresponds to the powers in Europe, NE_Asia, and N_America (from left to right), respectively, and time series are expressed as UTC+00.

It can be observed that a large share of energy supply for NE_Asia comes from solar PV thanks to the widely use of storage system that can shift surplus electricity. In contrast, Europe mainly utilizes electricity from onshore wind generation as there are abundant wind resources (higher CF) and onshore infrastructure cost is cheaper than that of offshore; also Europe locates generally at a higher latitude than the other two regions, thus less daytime for solar generation and lower regional CF.

Further insights can be found by analyzing the power interactions among three regions. As in Fig. 1 (c), during daytime of NE_Asia (2 am-11 am) in July, PV cells work at full capacity to generate electricity that is more than needed during this period. Part of the surplus energy is stored locally for later use and the remaining is exported to N_America where there is a shortage of locally generated electricity. During 1 pm - 1 am when NE_Asia stays at night, its neighbours currently at daytime export electricity back to NE_Asia, especially N_America, which shows the daily complementarity of renewable energy sources among regions, especially the solar generation. It is shown in Fig. 1(a) that compared to summer, PV cells produce less electricity (lower CF) while wind turbines generate more electricity (higher CF), which shows the seasonal complementarities of renewable generation.

The monthly electricity imports and exports of each region are summarized in Fig. 2, where positive and negative bar values represent import and export, respectively. The utilization factors of transmission interconnectors are shown in Fig. 4.

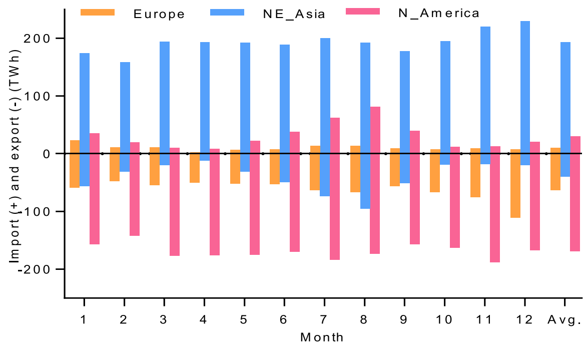

FIGURE 2. Monthly imports and exports of electricity.

As in Fig. 2, NE_Asia is dominated by the import (average 193 TWh, 16% of its demand) while Europe (11 TWh, 3%) and N_America (31 TWh, 6%) are dominated by the export. The reason is NE_Asia (14584 TWh) has nearly 1.5 times of the total demands of Europe (4216 TWh) and N_America (5846 TWh), and thus mass electricity is needed to maintain demand-supply balance compared to its neighbours. Fig. 4 shows that the annual utilization factors of transmission interconnectors 'Europe-NE_Asia', 'Europe-N_America' and 'NE_Asia-N_America' are roughly 46%, 54% and 53%, respectively.

C. SENSITIVITY ANALYSIS

In order to investigate how the capital cost per unit of storage system and transmission interconnector affects the economic benefits that interconnection would introduce, a set of scenarios are obtained to examine the interplay between the storage system and the transmission interconnector with respect to regional LCOE drop brought by interconnection.

The capital cost per unit of storage system and transmission interconnector are raised from 0.7x to 1.4x and 0.85x to 1.4x, respectively, according to [53], both with an interval of 0.05x (180 pairs in total). For each cost pair, regional LCOE as well as overall annual cost before and after the interconnection is calculated and the corresponding cost drop is finally obtained. It is worth noting that the optimal interconnection scheme is determined by the proposed planning model rather than being manually set. Fig. 3 gives the results of regional LCOE drop under different cost pairs, where red circles are several key points and asterisk is the value under basic settings of capital costs. The drop of overall LCOE and the interconnector capacities are shown in Fig. 5 and Fig. 6.

Fig.3 (a) shows that when the storage cost per unit is kept constant and transmission interconnector cost increases, the LCOE drop of NE_Asia declines continuously; when the storage cost is relatively low (e.g. 0.7x), above influence of line cost on LCOE is less sensitive. The reasons are as follows: when the installation of HVDC lines becomes more expensive, the local storage system plays an increasingly more important role in balancing supply and demand and thus the economic benefits of interconnection would be weakened.

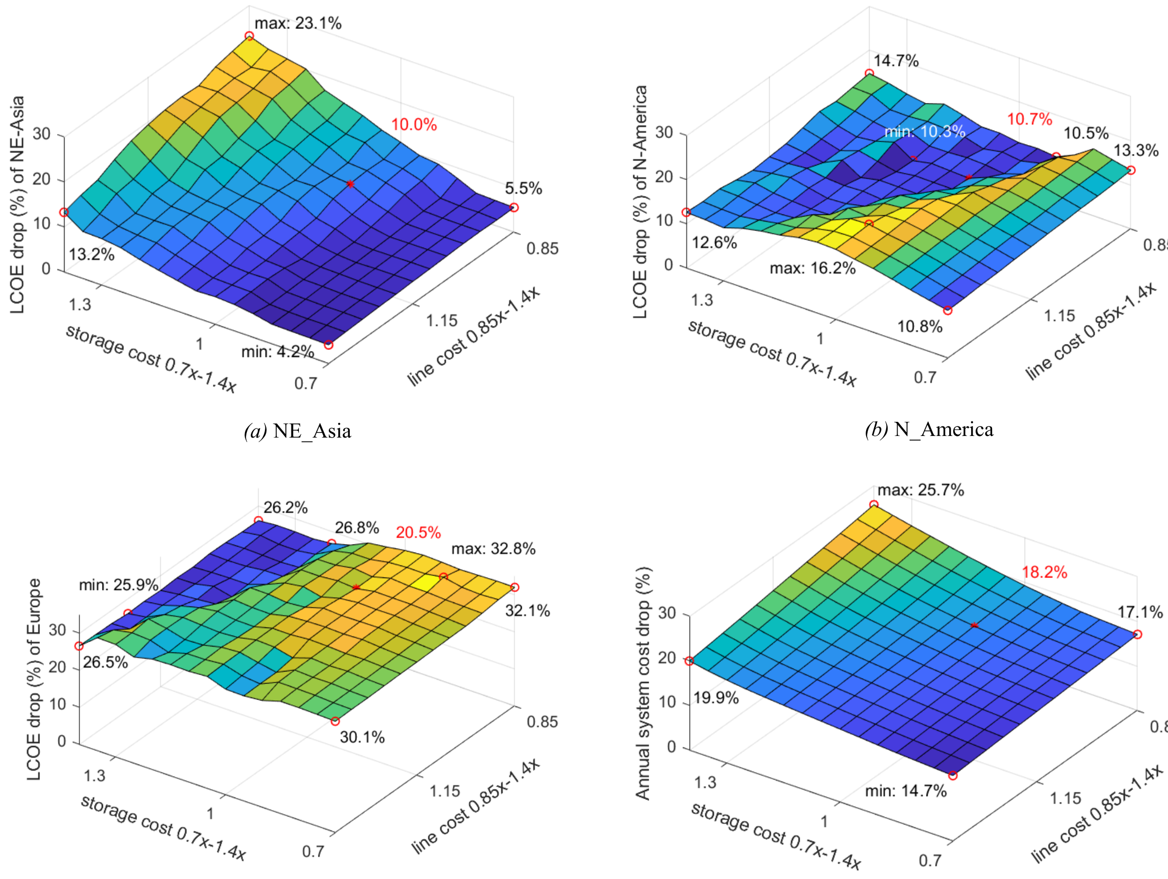

(a) NE_Asia

(b) N_America

(c) Europe

(d) Annual cost

FIGURE 3. Cost decrease under different cost pairs.

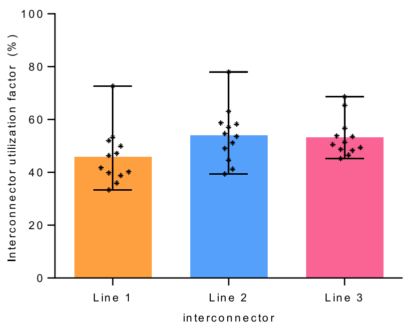

FIGURE 4. Transmission interconnector factors.

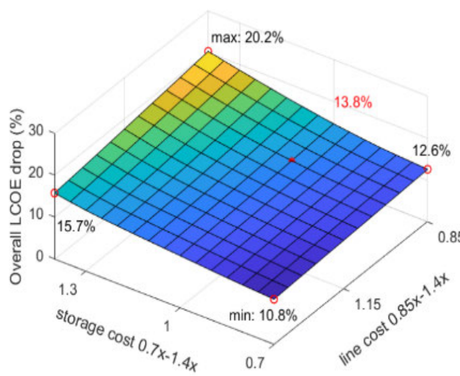

FIGURE 5. Overall LCOE decrease under different cost pairs.

Under constant transmission interconnector cost, the LCOE drop climbs with increasing storage cost. This is because higher storage system cost will lead to fewer energy storage installations, thus NE_Asia will rely more on neighbours to maintain system balance through transmission interconnectors. Furthermore, the LCOE drop shows less sensitivity to the cost of the transmission interconnector than that of the storage system because the investment in deploying HVDC interconnectors takes a much smaller share of the annual cost than deploying a storage system. Overall, with storage cost no less than 0.7x and line cost no more than 1.4x, the interconnection can yield a least 4% savings in NE_Asia's LCOE.

In Fig. 3 (b), the major difference is that under constant transmission interconnector cost and with increasing storage cost, the LCOE drop first climbs slightly then decreases and

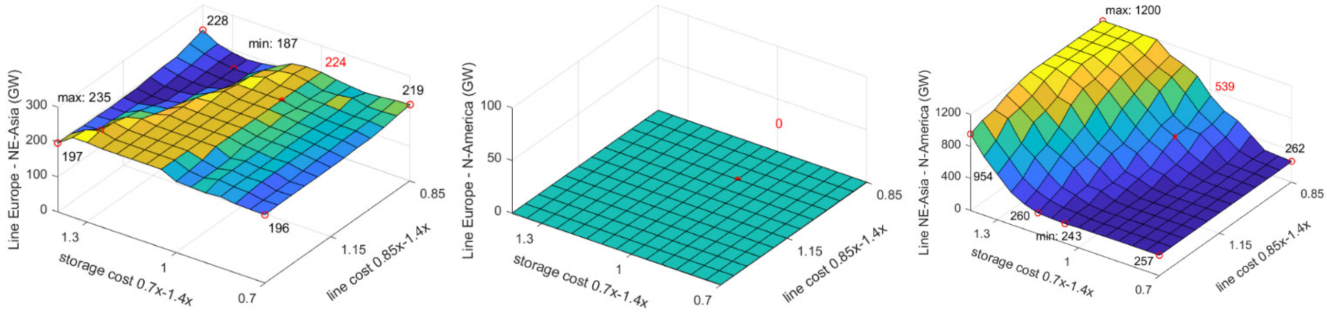

(a) Europe-NE_Asia (b) Europe-N_America (c) NE_Asia-N_America

FIGURE 6. Overall LCOE decrease under different cost pairs.

finally remains nearly stable. The lower the transmission interconnector cost, the longer the range for which the LCOE drop is kept stable. The reasons why LCOE drop keeps nearly unchanged are: N_America is dominated by export, which indicates redundant local installations of RE sources; the dispatch of those local generation sources can maintain the system balance easily and only the essential capacities of the storage system are needed, in this case, the capacities of storage system can hardly decrease much despite its cost per unit increasing and thus the interconnection can hardly yield further cost reductions. Overall, an approximate 10% of LCOE saving can be always achieved in N_America.

As shown in Fig. 3 (c), the LCOE drop of Europe shares similar varying trends with N_America. The difference is that the LCOE drop remains nearly unchanged for longer range at the beginning when the storage system cost climbs and the line cost is kept constant. Similarly, a reduction of 30% can be easily achieved and at least 26% is obtained.

From the perspective of annual system cost, it is shown in Fig. 3 (d) that at least a saving of 15% can be achieved regardless of the variable costs of storage system and transmission interconnector. Additionally, a least reduction of 11% can be achieved in terms of system overall LCOE (Fig. 5). The above sensitivity analysis demonstrates the necessity of interconnections among the three regions.

The proposed capacities of the transmission interconnectors, as in Fig. 6, are a minimum of 187 GW for Europe-NE_Asia, 243 GW for NE_Asia-N_America while the interconnection for Europe-N_America is not recommended, indicating that the interconnection between Europe grid and N_America grid is less beneficial. There are two primary reasons: the first is that the complementary effects between Europe and N_America are weaker than other pairs; second, the HVDC submarine power cable assumed to connect the two regions has a much higher capital cost per km than an overhead line.

The comparison of annual investment costs based on power series from 7 individual weather years and the representative series we employed is illustrated in Table 2.

As shown in Table 2, when different weather years are selected, the system annual cost varies a lot and the difference

TABLE 2. Annual cost based on different weather year.

Year	Annual cost (billion $) Before interconnection	After interconnection	Decrease (%)
2011	1068	844	21.0
2012	1009	886	12.3
2013	1021	819	19.8
2014	990	871	12.0
2015	1008	849	15.8
2016	1051	852	19.0
2017	982	801	18.4
Representative	1021	836	18.1

is about USD 86 billion (9%) for scenarios before the interconnection and USD 85 billion (11%) for those after the interconnection. Correspondingly, the saving of the total system annual cost that the interconnection yields varies from a low of 12% using 'Year 2014' to a high of 21% using 'Year 2011'. Additionally, the method of using representative series can generally cast a descent reflection of the resources availability within multi weather years in terms of the system annual cost and system overall LCOE as well as the cost reductions. For example, the annual cost after the interconnection is about USD 836 billion when the values based on individual years vary from USD 801 billion to USD 886 billion.

D. COMPLEMENTARY CHARACTERISTICS OF TIME DIFFERENCES

In this paper, the complementary characteristics of approximately 8-hour time differences between Europe, NE_Asia, and N_America are investigated first time. To achieve this, the time differences among three regions have to be eliminated but each region spans at least two time zones itself. It is therefore assumed that for each region, two scenarios of regional hourly demand/generation power series generated correspond to the two time zones, respectively. The results are summarized in Table 3.

As shown in Table 3, when there were no time differences being considered for Scenario 1 - 8, the transmission capacity of Europe-N_America would be at minimum 8 GW in all scenarios while those of the other two transmission interconnectors decrease, especially NE_Asia-N_America

TABLE 3. Annual cost for scenarios without time differences.

Scenario	Time zone (UTC) Europe	NE_Asia	N_America	Transmission (GW) L1[b]	L2	L3	Annual (billion $)	Inc[c] (%)
1	+0	+7	-7	209	8	192	872	4.2
2	+0	+7	-6	210	8	191	872	4.3
3	+0	+8	-7	205	8	186	869	3.9
4	+0	+8	-6	203	8	194	871	4.1
5	+1	+7	-7	209	8	201	872	4.2
6	+1	+7	-6	210	8	200	872	4.3
7	+1	+8	-7	211	8	187	870	4.0
8	+1	+8	-6	209	8	192	872	4.2
Ref.[a]	--	--	--	216	8	527	836	--

[a]'Ref.' means the reference scenario where time differences and the interconnection are considered, i.e, Scheme 7 in Table 1; [b]L1, L2, and L3 represent the interconnection of Europe-NE_Asia, Europe-N_America, and NE_Asia-N_America, respectively; [c] 'Inc' means the annual cost increase w.r.t the annual cost of 836 billion $ for Scheme 7 in Table 1.

where the capacity would drop by 63%; furthermore, the annual cost increase in cases without consideration of time differences is around 4% higher than that in the reference scenario with consideration of time differences.

E. N-1 SECURITY CONSIDERATION OF INTERCONNECTORS BETWEEN THREE REGIONS

For such macro scale interconnections between regions, it would be worth discussing the N-1 security consideration of interconnectors. In the light of N-1 security consideration, for the interconnectors between any pair of regions, one additional DC link needs to be added. For the sake of simple comparison, as a reference, Scheme 7 in Table 1 has a total annual cost of USD 836 billion. For Scheme 7, if N-1 security is considered, 3 additional DC lines will need to be added, and this will result in a total annual cost of USD 839 billion, which is just very slightly increased by 0.36% in comparison to that of USD 836 billion without the consideration of N-1 security.

V. CONCLUSION

In this study, massive historical weather data of up to 7 years at highly temporal and spatial resolution for Europe, North-East Asia, and North America have been downloaded, converted, selected, and aggregated to generate the representative power series of wind, and solar generation. An integrated planning model coupled with dispatch to determine the regional additional capacities of RE sources, storage systems and transmission interconnectors has been presented, where demands in 2050 are expected to be met by 100% renewable generation. A sensitivity analysis has been presented to validate the robustness of the results to variable infrastructure costs and to different weather years. The complementary characteristic of around 8-hour time differences between above three regions has been investigated for the first time.

The results have demonstrated that the interconnections reduce the overall installations of RE sources and storage systems and thus yield a saving of around 18% in annual system cost. Additionally, the regional LCOE will decrease by 31%, 10% and 10% for the Europe, NE_Asia and N_America, respectively where the interconnection capacities are 214 GW for Europe-NE_Asia, 8 GW for Europe-N_America, and 520 GW for NE_Asia-N_America, respectively.

TABLE 4. Geographical scope in this paper.

Region	No.[a]	Sub-area name
Europe	30	30 countries
North- East Asia	36	31 provinces in China plus Japan, South Korea, North Korea, Mongolia, and Far Eastern Federal District excluding Sakha Republic
North America	58	48 states in the USA except Alaska and Hawaii, 10 provinces in Canada at lower latitudes

[a] Total number of sub-areas in each region

TABLE 5. Expected installations in 2030 and installed potentials (GW).

	Expected in 2030 Europe	NE_Asia	N_America	Maximum installed potential Europe	NE_Asia	N_America
Onshore	255	453	333	1,909	5,393	5,311
Offshore	72	52	45	1,503	1,097	1,475
Solar	270	487	139	23,423	57,002	65,166
Hydro	139	475	200	324	640	393
Demand (TWh)	Europe: 4,216; NE_Asia:14,584; N_America: 5,846 (accounting for the transmission & distribution loss)					

See description below for references

TABLE 6. Sources of historical statistics

	Source and Website
Hydro	Eurosat: http://appsso.eurostat.ec.europa.eu/nui/show.do?dataset=nrg_105m
	Statistics Canada: https://www150.statcan.gc.ca/t1/tbl1/en/tv.action?pid=2510001501 EIA: https://www.eia.gov/electricity/data.php#generation
	National Bureau of Statistics: http://data.stats.gov.cn/easyquery.htm?cn=E0101
Load	ENTSO-e: https://tyndp.entsoe.eu/maps-data
	EIA: https://www.eia.gov/todayinenergy/detail.php?id=27212 ESO: Alberta, British Columbia, New Brunswick, Ontario
	Japan power companies websites: Chubu, Chugoku, Hokkaido, Hokuriku, Kansai, Kyushu, Shikoku, Tohoku, Tokyo NDRC: http://www.gov.cn/xinwen/2019-12/30/content_5465088.htm

Sensitivity analysis shows that at least a reduction of 26% for Europe, 4% for NE_Asia, and 10% for N_America, along with 15% for annual cost can be achieved after the interconnections are deployed, despite variable infrastructure costs. Although resources availability of different weather years influences the system investment costs, the interconnection can always bring an annual cost saving.

When there were no time differences, the transmission capacity of Europe-N_America would be at minimum 8 GW in all scenarios while those of the other two transmission interconnectors decrease, especially NE_Asia-N_America where the capacity would drop by 63%; furthermore, the annual cost increase in cases without consideration of time differences would be around 4% higher than that in the reference scenario with consideration of time differences, which indicates the benefits of time difference related complementary effects of continental power grid interconnections.

TABLE 7. Monthly regional capacity factors of different technologies (%).

	Solar PV			Onshore wind			Offshore wind			Hydro		
	Europe	NE_ Asia	N_ America	Europe	NE_ Asia	N_ America	Europe	NE_ Asia	N_ America	Europe	NE_ Asia	N_ America
Jan.	7.45	17.07	12.00	41.71	27.56	42.43	59.84	51.69	50.25	39.34	29.19	57.65
Feb.	10.96	20.22	16.35	41.60	30.21	43.06	60.92	46.23	47.90	36.48	27.70	51.13
Mar.	16.57	23.38	20.52	39.13	32.42	43.60	54.29	40.64	49.22	39.23	29.13	54.83
April	20.57	24.95	22.96	34.22	32.38	42.95	50.64	42.59	47.04	35.11	30.59	50.29
May	21.92	24.76	23.66	29.01	30.63	35.57	43.89	36.15	38.57	38.29	39.27	50.59
June	22.70	23.27	24.04	25.85	21.46	33.31	40.28	31.45	37.68	37.23	45.93	49.64
July	22.66	22.48	24.06	21.94	20.00	28.88	35.39	34.21	31.59	34.31	54.71	47.61
Aug.	20.88	22.08	22.49	23.68	19.05	24.78	39.72	27.48	28.51	31.43	54.10	43.69
Sept.	16.41	21.12	19.69	29.70	21.74	33.64	46.68	31.47	39.47	30.36	51.32	38.75
Oct.	12.14	19.53	15.74	35.51	26.46	40.70	58.51	46.27	46.88	34.50	48.15	38.95
Nov.	8.11	16.22	12.30	38.23	29.81	42.59	58.34	48.10	49.50	37.34	37.52	43.98
Dec.	6.45	15.36	10.07	44.16	27.57	42.70	65.08	53.69	48.65	38.37	30.56	51.07
Ann.[a]	**15.57**	**20.87**	**18.66**	**33.73**	**26.61**	**37.85**	**51.13**	**40.83**	**42.94**	**36.00**	**39.85**	**48.18**

[a] 'Ann.' means the annual capacity factor

TABLE 8. Installed cost per unit of different interconnector types.

HVDC Type	Line ($/km/MW)	Converter pair ($/kW)	Transmission loss	
			Line (%/1000km)	Converter pair (%/pair)
±1100	142	202	1.60%	1.4%
±800	875	228	1.60%	1.4%

1$ = 6.6￥, 1€ = 7.7￥ (2019); See description below for references.

TABLE 9. Information about transmission lines.

Interconnector	Terminals		Distance (km)	Type	Voltage (kV)	Total loss (%)
	Terminal 1	Terminal 2				
Europe-NE_Asia	Berlin	Urumqi	5353	Overhead line	± 1100	9.96
Europe-N_America	Great Britain	Newfoundland and Labrador	3300	Submarine cable	± 800	6.68
NE_Asia-N_America	Khabarovsk	Portland	7759	Overhead line	± 1100	13.81

See description below for references.

TABLE 10. Regional financial assumptions for technologies and operational parameters.

Technology	Financial assumptions				Limit
	Item	Unit	2030	2040	min, max
Utility PV	Capital	$/kW	321	238	0, 1
	O&M fix	%/year	2.33	2.45	
	O&M var	$/kWh	0	0	
	Lifetime	year	30	30	
On -shore	Capital	$/kW	1075	950	0, 1
	O&M fix	%/year	1.90	1.90	
	O&M var	$/kWh	0	0	
	Lifetime	year	25	25	
Off -shore	Capital	$/kW	2450	2275	0, 1
	O&M fix	%/year	2.80	2.80	
	O&M var	$/kWh	0	0	
	Lifetime	year	25	25	
Hydro	Capital	$/kW	1704	1704	0, 1
	O&M fix	%/year	1.50	1.50	
	O&M var	$/MWh	5.83	5.83	
	Lifetime	year	40	40	
Li-Battery	Capital	$/kWh	137	93	0, 1; Efficiency: 0.95; Energy-to-power: 4h τ =0
	O&M fix	%/year	2.31	2.75	
	O&M var	$/MWh	0.23	0.23	
	Lifetime	year	15	15	

See description below for references.

It should be emphasized herein that the relatively lower projected cost data are used for Solar and Energy Storage while the cost data used for UHVDC are taken from recent projects and assumed to be unchanged in the future. This would encourage more local installations of solar and energy storage rather than interconnectors, which will lead to conservative results for interconnections. In addition, the total cost with N-1 security consideration of 3 interconnections has been just slightly increased by 0.36% in comparison to that without the consideration of N-1 security.

This paper has been focused on the benefits of integration via transmission links to show the merits of taking advantage of complementarities and a novel analysis of how a global interconnected system would behave has been discussed. However, this paper has not considered the power grid modeling at national level. In the future work, it would be useful to consider a more detailed model of national grids and hence the power flows between national grids within a region. A well-known open question for any power system expansion planning problem is how to deal with future uncertainties effectively. The basic principle is to use the up-to-date projected generation and demand data, detailed network models, and most recent international and national energy policies available as well as the latest technological & market developments. Given the international drive towards a net-zero strategy, further research is needed to refine the novel models developed in this paper.

APPENDIX

Notes for references in Tables.

Table 5: The regional expected installations in 2030 come from [54]–[56] for NE_Asia, from IRENA for Europe and N_America. Hydro potentials are taken from [57], [58]. The regional expected annual demands in 2050 are from [4]. *Table 8/9*: The interconnection routes and investment costs are from [30]–[32], [59] and [60], [61], respectively. *Table 10*: The costs for 2040 were fed into the model [15]. All the regions are assumed to share the same assumptions. Information of PV and batteries are from [4], [53]. Those of wind generation are from [4, 62].The hydro cost is set as the global weighted average installed cost in 2019 [63].

TABLE 11. Additional annual costs of different technologies in each region (billion $).

Scheme	Solar			Wind onshore			Wind offshore			Hydro			Storage		
	Europe	NE_Asia	N_America	Europe	NE_Asia	N_America	Europe	NE_Asia	N_America	Europe	NE_Asia	N_America	Europe	NE_Asia	N_America
0	20	273	56	106	0	31	43	0	0	28	0	32	18	343	72
1	20	178	56	106	127	31	0	0	0	0	0	32	21	260	72
2	33	273	25	77	0	107	22	0	0	29	0	30	25	343	23
3	20	224	23	148	2	146	43	0	0	28	1	0	18	271	12
4	19	205	57	69	17	107	0	0	0	29	1	0	13	239	19
5	33	169	72	95	37	94	0	0	0	0	1	0	17	197	39
6	26	173	38	113	85	57	0	0	0	0	1	31	8	249	23
7	33	170	73	95	38	91	0	0	0	0	1	0	15	201	39

TABLE 12. Proposed installed capacities of different technologies in each region including existing capacities In 2030 (GW).

Scheme	Solar			Wind onshore			Wind offshore			Hydro			Storage (GWh)		
	Europe	NE_Asia	N_America	Europe	NE_Asia	N_America	Europe	NE_Asia	N_America	Europe	NE_Asia	N_America	Europe	NE_Asia	N_America
0	1,053	11,421	2,396	1,315	453	641	238	52	45	324	475	393	1,365	26,545	5,563
1	1,073	7,612	2,396	1,321	1,727	641	72	52	45	139	475	393	1,628	20,149	5,563
2	1,573	11,421	1,141	803	453	1,410	158	52	45	324	475	393	1,956	26,545	1,754
3	1,053	9,445	1,073	1,315	471	1,805	238	52	45	324	475	200	1,365	20,947	921
4	1,038	8,685	2,435	944	629	1,403	72	52	45	324	475	200	977	18,510	1,478
5	1,603	7,231	3,023	1,212	825	1,281	72	52	45	139	475	200	1,328	15,269	3,031
6	1,307	7,388	1,650	1,388	1,304	908	72	52	45	139	475	393	623	19,259	1,779
7	1,579	7,297	3,049	1,214	831	1,246	72	52	45	139	475	200	1,162	15,553	3,025

REFERENCES

[1] *Paris Agreement*, United Nations, New York, NY, USA, 2015.

[2] *Global Energy Transformation: A Roadmap to 2050*, IRENA, Abu Dhabi, United Arab Emirates, 2019.

[3] M. Z. Jacobson *et al.*, ''Impacts of green new deal energy plans on grid stability, costs, jobs, health, and climate in 143 countries,'' *One Earth*, vol. 1, no. 4, pp. 449–463, Dec. 2019.

[4] D. Bogdanov *et al.*, ''Radical transformation pathway towards sustainable electricity via evolutionary steps,'' *Nature Commun.*, vol. 10, no. 1, pp. 1–16, Dec. 2019.

[5] Z. Liu, *Ultra-High Voltage AC/DC Grids*. New York, NY, USA: Academic, 2014.

[6] M. Ardelean and P. Minnebo, ''HVDC submarine power cables in the world: State-of-the-art knowledge,'' Joint Res. Center, Ispra, Italy, Tech. Rep. EUR27527EN, 2015.

[7] S. Chatzivasileiadis, D. Ernst, and G. Andersson, ''The global grid,'' *Renew. Energy*, vol. 57, pp. 372–383, Sep. 2013.

[8] Z. Liu, *Global Energy Interconnection*. Amsterdam, The Netherlands: Elsevier, 2015.

[9] H. Liu, G. B. Andresen, and M. Greiner, ''Cost-optimal design of a simplified highly renewable Chinese electricity network,'' *Energy*, vol. 147, pp. 534–546, Mar. 2018.

[10] M. Esteban *et al.*, ''100% renewable energy system in Japan: Smoothening and ancillary services,'' *Appl. Energy*, vol. 224, pp. 698–707, Aug. 2018.

[11] K. Hansen, B. V. Mathiesen, and I. R. Skov, ''Full energy system transition towards 100% renewable energy in Germany in 2050,'' *Renew. Sustain. Energy Rev.*, vol. 102, pp. 1–13, Mar. 2019.

[12] B. Elliston, M. Diesendorf, and I. MacGill, ''Simulations of scenarios with 100% renewable electricity in the Australian national electricity market,'' *Energy Policy*, vol. 45, pp. 606–613, Jun. 2012.

[13] F. Zickfeld *et al.*, ''Desert power 2050: Perspectives on a sustainable power system for EUMENA,'' Dii GmbH, 2012. [Online]. Available: http://www.desertec-uk.org.uk/reports/DII/DPP_2050_Study.pdf

[14] D. Bogdanov and C. Breyer, ''North-east asian super grid for 100% renewable energy supply: Optimal mix of energy technologies for electricity, gas and heat supply options,'' *Energy Convers. Manage.*, vol. 112, pp. 176–190, Mar. 2016.

[15] W. Zappa, M. Junginger, and M. van den Broek, ''Is a 100% renewable European power system feasible by 2050?'' *Appl. Energy*, vols. 233–234, pp. 1027–1050, Jan. 2019.

[16] A. Aghahosseini, D. Bogdanov, L. S. N. S. Barbosa, and C. Breyer, ''Analysing the feasibility of powering the Americas with renewable energy and inter-regional grid interconnections by 2030,'' *Renew. Sustain. Energy Rev.*, vol. 105, pp. 187–205, May 2019.

[17] D. P. Schlachtberger, T. Brown, S. Schramm, and M. Greiner, ''The benefits of cooperation in a highly renewable European electricity network,'' *Energy*, vol. 134, pp. 469–481, Sep. 2017.

[18] M. Z. Jacobson *et al.*, ''100% clean and renewable wind, water, and sunlight all-sector energy roadmaps for 139 countries of the world,'' *Joule*, vol. 1, no. 1, pp. 108–121, Sep. 2017.

[19] D. Connolly, H. Lund, and B. V. Mathiesen, ''Smart energy Europe: The technical and economic impact of one potential 100% renewable energy scenario for the European Union,'' *Renew. Sustain. Energy Rev.*, vol. 60, pp. 1634–1653, Jul. 2016.

[20] T. W. Brown, T. Bischof-Niemz, K. Blok, C. Breyer, H. Lund, and B. V. Mathiesen, ''Response to 'burden of proof: A comprehensive review of the feasibility of 100% renewable-electricity systems,''' *Renew. Sustain. Energy Rev.*, vol. 92, pp. 834–847, Sep. 2018.

[21] M. Diesendorf and B. Elliston, ''The feasibility of 100% renewable electricity systems: A response to critics,'' *Renew. Sustain. Energy Rev.*, vol. 93, pp. 318–330, Oct. 2018.

[22] R. B. Fuller and K. Kuromiya, *Critical Path*. New York, NY, USA: Macmillan, 1981.

[23] Y. Rudenko and V. Yershevich, ''Is it possible and expedient to create a global energy network?'' *Int. J. Global Energy Issues*, vol. 3, no. 3, pp. 159–165, 1991.

[24] *Electric Power Grid Interconnections in the APEC Region*, Asia Pacific Energy Res. Center, Tokyo, Japan, 2004.

[25] M. Kanagawa and T. Nakata, ''Analysis of the impact of electricity grid interconnection between Korea and Japan—Feasibility study for energy network in Northeast Asia,'' *Energy Policy*, vol. 34, no. 9, pp. 1015–1025, Jun. 2006.

[26] Y. Shu and W. Chen, ''Research and application of UHV power transmission in China,'' *High Voltage*, vol. 3, no. 1, pp. 1–13, Mar. 2018.

[27] K. Schaber, F. Steinke, and T. Hamacher, ''Transmission grid extensions for the integration of variable renewable energies in Europe: Who benefits where?'' *Energy Policy*, vol. 43, pp. 123–135, Apr. 2012.

[28] S. Spiecker, P. Vogel, and C. Weber, ''Evaluating interconnector investments in the north European electricity system considering fluctuating wind power penetration,'' *Energy Econ.*, vol. 37, pp. 114–127, May 2013.

[29] A. Boute and P. Willems, ''RUSTEC: Greening Europe's energy supply by developing Russia's renewable energy potential,'' *Energy Policy*, vol. 51, pp. 618–629, Dec. 2012.

[30] M. Ardelean and P. Minnebo, ''A China-EU electricity transmission link: Assessment of potential connecting countries and routes,'' Joint Res. Center, Ispra, Italy, Tech. Rep. EUR29098EN, 2017.

[31] A. Purvins, L. Sereno, M. Ardelean, C.-F. Covrig, T. Efthimiadis, and P. Minnebo, ''Submarine power cable between Europe and North America: A techno-economic analysis,'' *J. Cleaner Prod.*, vol. 186, pp. 131–145, Jun. 2018.

[32] GEIDCO. (2018). *Global Energy Interconnection Backbone Grid Research*. [Online]. Available: http://globalsmartgridfederation.org/page/480/world-global-energy-interconnection-backbone-grid-research
[33] *China's Grid Architect Proposes a 'Made in China' Upgrade to North America's Power System*. Accessed: Sep. 2019. [Online]. Available: https://spectrum.ieee.org/energywise/energy/renewables/chinas-grid-architect-offers-made-in-china-upgrade-to-north-americas-power-system
[34] *EuroAsia Interconnector*. Accessed: Oct. 2019. [Online]. Available: https://www.euroasia-interconnector.com/
[35] M. Brinkerink, B. Ó. Gallachóir, and P. Deane, "A comprehensive review on the benefits and challenges of global power grids and intercontinental interconnectors," *Renew. Sustain. Energy Rev.*, vol. 107, pp. 274–287, Jun. 2019.
[36] J. Yu *et al.*, "Global electricity network-feasibility study," CIGRE, Tech. Rep. 775, 2019.
[37] G. B. Andresen, A. A. Søndergaard, and M. Greiner, "Validation of Danish wind time series from a new global renewable energy atlas for energy system analysis," *Energy*, vol. 93, pp. 1074–1088, Dec. 2015.
[38] J. Hörsch, F. Hofmann, D. Schlachtberger, and T. Brown, "PyPSA-Eur: An open optimisation model of the European transmission system," *Energy Strategy Rev.*, vol. 22, pp. 207–215, Nov. 2018.
[39] H. Liu, T. Brown, G. B. Andresen, D. P. Schlachtberger, and M. Greiner, "The role of hydro power, storage and transmission in the decarbonization of the Chinese power system," *Appl. Energy*, vol. 239, pp. 1308–1321, Apr. 2019.
[40] ECMWF. *ERA5*. Accessed: Mar. 2020. [Online]. Available: https://www.ecmwf.int/en/forecasts/datasets/reanalysis-datasets/era5
[41] IHO and UNESCO. *Gridded Bathymetry Data*. Accessed: Mar. 2020. [Online]. Available: https://www.gebco.net/data_and_products/gridded_bathymetry_data/
[42] *GADM Maps and Data*. Accessed: Mar. 2020. [Online]. Available: https://gadm.org/index.html
[43] NACIS. *Natural Earth: Free Vector and Raster Map Data*. Accessed: Mar. 2020. [Online]. Available: https://www.naturalearthdata.com/
[44] OEP. *Wind Turbine Library*. Accessed: May 2020. [Online]. Available: https://openenergy-platform.org/dataedit/view/supply/wind_turbine_library
[45] T. Huld, R. Gottschalg, H. G. Beyer, and M. Topić, "Mapping the performance of PV modules, effects of module type and data averaging," *Sol. Energy*, vol. 84, no. 2, pp. 324–338, Feb. 2010.
[46] E. Schubert, J. Sander, M. Ester, H. P. Kriegel, and X. Xu, "DBSCAN revisited, revisited: Why and how you should (still) use DBSCAN," *ACM Trans. Database Syst.*, vol. 42, no. 3, pp. 1–21, Aug. 2017.
[47] *FUTURE OF SOLAR: Deployment, Investment Technology, Grid Integration and Socio-Economic Aspects*, IRENA, Abu Dhabi, United Arab Emirates, 2019.
[48] *Cost Projections for Utility-Scale Battery Storage*, NREL, Golden, CO, USA, 2019.
[49] *Grid Energy Storage Technology Cost and Performance Assessment*, United States Dept. Energy, Washington, DC, USA, 2020.
[50] M. Gan, H.-X. Li, C. L. P. Chen, and L. Chen, "A potential method for determining nonlinearity in wind data," *IEEE Power Energy Technol. Syst. J.*, vol. 2, no. 2, pp. 74–81, Jun. 2015.
[51] C. Opathella, A. Elkasrawy, A. A. Mohamed, and B. Venkatesh, "Optimal scheduling of merchant-owned energy storage systems with multiple ancillary services," *IEEE Open Access J. Power Energy*, vol. 7, pp. 31–40, 2020.
[52] W. Wei, D. Wu, Z. Wang, S. Mei, and J. P. S. Catalão, "Impact of energy storage on economic dispatch of distribution systems: A multi-parametric linear programming approach and its implications," *IEEE Open Access J. Power Energy*, vol. 7, pp. 243–253, 2020.
[53] E. Vartiainen, G. Masson, C. Breyer, D. Moser, and E. R. Medina, "Impact of weighted average cost of capital, capital expenditure, and other parameters on future utility-scale PV levelised cost of electricity," *Prog. Photovolt., Res. Appl.*, vol. 28, no. 6, pp. 439–453, Jun. 2020.
[54] *China Energy Outlook 2030 (in Chinese)*, Energy Res. Inst., Wuhan, China, 2016.
[55] *Japan: Greater Energy Security Through Renewables*, IEEFA, Cleveland, OH, USA, 2017.
[56] *Renewable Energy 3020 Plan*, MOTIE, Sejong City, South Korea, 2017.
[57] *Technology Roadmap: Hydropower*, IEA, Paris, France, 2012.
[58] *World Energy Resources: Hydropowr|2016*, World Energy Council, London, U.K., 2016.
[59] P. Meisen, "The potential of an electrical interconnection between Russia and North America," Global Energy Netw. Inst., Jan. 1992. Accessed: Jan. 9, 2019.
[60] X. Zhao *et al.*, "Technical and economic demands of HVDC submarine cable technology for global energy interconnection," *Global Energy Interconnection*, vol. 3, no. 2, pp. 120–127, Apr. 2020.
[61] Z. Q. Zhao, Y. M. Dai, X. F. Song, L. C. Sun, and H. Z. Nie, "Research on the economy of UHVDC transmission under the background of global energy interconnect," *IOP Conf. Ser., Mater. Sci. Eng.*, vol. 439, Nov. 2018, Art. no. 052022.
[62] *FUTURE OF WIND: Deployment, Investment Technology, Grid Integration and Socio-Economic Aspects*, IRENA, Abu Dhabi, United Arab Emirates, 2019.
[63] *Renewable Power Generation Costs in 2019*, IRENA, Abu Dhabi, United Arab Emirates, 2020.

CONG WU received the B.Eng. and M.Sc. degrees in electrical engineering from China Agricultural University, Beijing, China, in 2015 and 2017, respectively. He is currently pursuing the Ph.D. degree with the University of Birmingham, Birmingham, U.K. His research interests include transcontinental electricity interconnection, and optimal power flow.

XIAO-PING ZHANG (Fellow, IEEE) is currently a Professor of Electrical Power Systems with the University of Birmingham, U.K. He is also the Director of Smart Grid with the Birmingham Energy Institute and the Co-Director of the Birmingham Energy Storage Center. He has coauthored the first and second edition of the monograph *Flexible AC Transmission Systems: Modeling and Control* published by Springer in 2006 and 2012. He has also coauthored the book *Restructured Electric Power Systems: Analysis of Electricity Markets with Equilibrium Models* published by IEEE Press/Wiley in 2010. His research interests include modeling and control of HVDC, FACTS, and wind/wave generation, distributed energy systems and market operations, and power system planning. He has been made a Fellow of IEEE "for contributions to modeling and control of high-voltage DC and AC transmission systems." He is also an IEEE PES Distinguished Lecturer on HVDC, FACTS, and Wave Energy Generation. He is also a Fellow of IET. He has been the Advisor to IEEE PES U.K. & Ireland Chapter and chairing the IEEE PES WG on Test Systems for Economic Analysis. He has been appointed recently to the Expert Advisory Group of U.K. Government's Offshore Transmission Network Review.

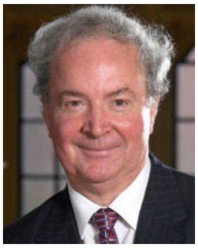

MICHAEL J. H. STERLING received the B.Eng. degree (Hons.) in electronic and electrical engineering from The University of Sheffield, U.K., in 1968, and the Ph.D. degree in computer control of power systems in 1971 and the D.Eng. degree in 1988. In 1971, he joined the Department of Control Engineering, The University of Sheffield, as a Lecturer, being promoted to a Senior Lecturer in 1978. In 1980, he was appointed as a Professor with the University of Durham, U.K., before being appointed the Vice-Chancellor and the Principal of Brunel University in 1990. He subsequently became the Vice Chancellor of the University of Birmingham in 2001 retiring in 2009 as one of the U.K.'s longest serving university leaders. He is also a Fellow of the Institution of Engineering and Technology, the Institute of Measurement and Control, and the Royal Academy of Engineering. He was a member of the U.K. Prime Minister's Council for Science and Technology from 2003 to 2013, where he was also the Chair of the Energy Group. He has served as the chairman for many organizations, most recently of the Science and Technology Facilities Council from 2009 to 2018.